Statistical Moments of Reaction Rates in Subsurface Reactive Solute Transport

X. Sanchez-Vila, A. Guadagnini, M. Dentz and D. Fernàndez-Garcia

Abstract Transport of reactive species in the subsurface is driven by mixing processes. Quantification of the mixing rate is, therefore, the basis for a proper characterization of the fate of pollutants in geochemically active environments. We consider the case of an anisotropic correlated random field, with perfect correlation in the horizontal plane, while the vertical integral scale is finite. Flow is uniform and takes place in the x-direction. Longitudinal constant dispersion is considered. Based on the analytical results of De Simoni et al. (2005) for the evaluation of reaction rates at the local scale, reaction is driven by local dispersion at any given point in space and time. Still, due to uncertainty in the advective velocity, reaction rates become a Spatial and Temporal Random Function. The aim of the work is to find the statistical moments of reaction rates, which in this particular configuration can be obtained exactly.

1 Introduction

Mixing has been recognized as the controlling process in several problems dealing with transport of reactive species in the subsurface. Mixing of two waters under perfect geochemical equilibrium with the natural porous medium would produce a local disequilibrium. A reaction will then take place to equilibrate the system. The types of reactions include precipitation/dissolution, adsorption/desorption, redox, and acid/base, amongst others. Appropriate quantification of the mixing rate is key for a proper characterization of solute spreading in geochemically active heterogeneous environments, with important implications in a number of environmental applications, including aquifer remediation schemes.

X. Sanchez-Vila
Department of Geotechnical Engineering and Geosciences, Technical University of Catalonia, Campus Nord D2-006, 08034 Barcelona, Spain
e-mail: xavier.sanchez-vila@upc.edu

A. Soares et al. (eds.), *geoENV VI – Geostatistics for Environmental Applications*, 127–139

Recently a methodology was presented to evaluate solute concentrations and reaction rates when homogeneous reactions (between aqueous species) or heterogeneous reactions (involving both aqueous species and the solid phase) take place under chemical equilibrium conditions (De Simoni et al., 2005). This methodology allows for the derivation of exact analytical expressions, applicable at the local scale, where mixing is mainly driven by diffusion or local dispersion. The salient question then becomes how to further elaborate on these results in order to obtain predictions of reaction rates in randomly heterogeneous media, together with a quantification of the associated uncertainty.

Our approach consists of the following steps. First, we define the geochemical problem. In this case, we consider a reaction of pure precipitation/dissolution, involving two aqueous species at equilibrium with an immobile solid mineral. Second, the flow and transport problems are formulated. These take place within a three-dimensional randomly heterogeneous, statistically uniform, hydraulic conductivity field, K, of infinite lateral extent. Hydraulic conductivity is isotropic at the local scale, but highly anisotropic in terms of correlation distances. The range of the conductivity variogram is very large (theoretically infinite) in the two horizontal directions, while it is finite along the vertical. This model is often employed to provide a depiction of a statistically stratified medium, where layering is not described in terms of a vertical sequence of disjoint materials, but rather as a continuous transition between different values of K, that are variably correlated along the vertical. A uniform head gradient is imposed parallel to the direction of layering. The (random) reaction rates are then computed exactly at the local scale as a function of the random K, following the methodology of De Simoni et al. (2005). It is then possible to compute the main statistics of the reaction rate, in terms of a simple quadrature in the probabilistic space from which hydraulic conductivity values are sampled. We concentrate on the first two statistical moments, and provide some ideas on the conditions where the ensemble values are actually a good representation of the real physical values.

2 Problem Statement

2.1 The Geochemical Problem

We consider the geochemical problem of the so-called bi-species system (Gramling et al., 2002; De Simoni et al., 2005). This involves the presence of two aqueous solutes, B_1 and B_2, which are in chemical equilibrium with a solid mineral, M_3. Without loss of generality we consider the case in which both stoichiometric coefficients are equal to one and the immobile solid mineral dissolves reversibly to yield species B_1 and B_2:

$$B_1 + B_2 \Leftrightarrow M_3. \tag{1}$$

In this particular case, the mass action law implies that the two aqueous species must satisfy at all points and all times the following condition

$$c_1 c_2 = K_{eq}, \tag{2}$$

where K_{eq} is the equilibrium constant, which is a function of temperature, pressure and chemical composition of the solution. In (2) we assume implicitly that activity coefficients are equal to 1. If at any given moment in space or time two waters satisfying (2) are put in contact, it is easily proven that the mixed water will not satisfy the equilibrium condition anymore (i.e., immediately it occurs that $c_{1,m}c_{2,m} > K_{eq}$, $c_{1,m}$ and $c_{2,m}$ respectively being the concentration of B_1 and B_2 in the mixed water). Under these circumstances precipitation takes place instantaneously and concentrations c_i $(i = 1, 2)$ are reduced in equal proportions, until (2) is again satisfied.

2.2 Geostatistical Model for Hydraulic Conductivity and Flow Set-up

We model hydraulic conductivity, K, as a three-dimensional stationary random space function, with mean $\langle K \rangle$ and variance σ_K^2. The two-point covariance of K is of axisymmetric anisotropy and is modeled with an exponential variogram $\gamma_K(\mathbf{h}) \equiv \gamma_K(h_1, h_2, h_3) = \sigma_K^2 \exp\left(-\left(\frac{h_1^2}{\lambda_1^2} + \frac{h_2^2}{\lambda_2^2} + \frac{h_3^2}{\lambda_3^2}\right)^{1/2}\right)$. Here, h_1, h_2, h_3 are separation distances along directions x,y, and z, respectively; λ_1, λ_2 $(= \lambda_1)$, λ_3 are measures of the corresponding correlation scales. The adopted assumption of stationarity implies that the probability density function (pdf) of K, p_K, be invariant under translation within the system.

We then consider one of the simplest models of heterogeneity, which is that of stratified formations. According to this model, K varies only in the vertical direction, z. Interest in this model has been motivated by its simplicity and by the recognition of the importance of layering upon solute transport in sedimentary formations (e.g. Matheron and de Marsily, 1980). Its simplicity allows grasping the key features of transport processes that can be recognized in more complex systems. From a practical viewpoint, we note that, although perfect layering is rarely found over large horizontal distances, the model can be applied to depict transport of contaminants over relatively short travel times.

In this work, layering is modeled in a geostatistical sense, i.e., we consider that λ_1, $\lambda_2 \to \infty$, while λ_3 is finite. We consider a saturated groundwater flow that is parallel to the direction of bedding. In other words, flow is driven by a constant horizontal gradient, $\boldsymbol{J}$, that is aligned along the x-direction ($\boldsymbol{J} = (J,0,0)$). We further assume the flow domain to be of large lateral extent, so that boundary effects can be disregarded. As a consequence, the steady-state Darcy's velocities at any point in the domain, $q(z)$, are given by

$$q(z) = -K(z)J. \tag{3}$$

Here, we note that J is negative, so that flow takes place in the direction of increasing x.

2.3 The Transport Equations

The mass balance equations for the two aqueous species are

$$\phi \frac{\partial c_i}{\partial t} = JK \frac{\partial c_i}{\partial x} + \phi D_L \frac{\partial^2 c_i}{\partial x^2} + w_e c_{e,i} - r \quad i = 1, 2, \tag{4}$$

where ϕ [–] is porosity, D_L [L^2T^{-1}] is the local scale longitudinal diffusion-dispersion value, w_e [T^{-1}] is an external recharge contribution, and $c_{e,i}$ [ML^{-3}] are the concentrations of species B_i in the recharging water. In this paper we concentrate on a diffusion coefficient which is constant and independent on local velocity. The problem could be made more general by adding an additional term accounting for a dispersion coefficient, but the main conclusions of the paper would not change.

Defining c_3 as the concentration of the mineral, the reaction rate, r [$ML^{-3}T^{-1}$] is incorporated as a sink/source term in the right hand side of (4), given as

$$\frac{\partial c_3}{\partial t} = r. \tag{5}$$

In (4) we have discarded the impact of the transverse dispersion, D_T, that causes mixing along the y-direction and between (statistically defined) layers. The reason is that we are interested in exploring the early-time behavior of the system, i.e., processes occurring within the regime for which $(tD_T)/\lambda_3^2 << 1$. In these scenarios, the effect of tranverse dispersivity has not yet developed in the system (Dentz and Carrera, 2003) and can be neglected in the governing equation.

Following the methodology of De Simoni et al. (2005), the system can be fully defined in terms of a conservative components, **u**, defined as stoichiometric combinations of the aqueous concentrations. In the bi-species system presented here, where the precipitation/dissolution reaction involves equal stoichiometric coefficients, a single component is needed, defined as

$$u = c_1 - c_2. \tag{6}$$

This component is advected and dispersed according to a transport equation that can be derived by subtracting the two transport equations in (4), leading to

$$\phi \frac{\partial u}{\partial t} = JK \frac{\partial u}{\partial x} + \phi D_L \frac{\partial^2 u}{\partial x^2} + w_e u_e. \tag{7}$$

The solution for u depends on the boundary and initial conditions of the problem to be solved. Combining (6) and the mass action law (2), it is possible to write the concentrations c_i explicitly, in terms of u (speciation process)

$$c_1 = \frac{u + \sqrt{u^2 + 4K_{eq}}}{2}; \quad c_2 = \frac{-u + \sqrt{u^2 + 4K_{eq}}}{2}. \tag{8}$$

Even though K_{eq} displays variations with temperature or salinity, in many groundwater-related geochemical processes we can assume that $K_{eq} \cong$ constant. In such a case, the aqueous concentrations are only functions of $u(i.e., c_i = f(u))$. Based on the method of De Simoni et al. (2005), it is possible to derive a closed-form expression for the reaction rate. The method consists of expanding (4) for one of the species, and then developing the spatial and temporal derivatives of c_i using the chain rule. We finally simplify the resulting expression by means of (7) and derive the following expression for the reaction rate,

$$r = \phi D_L \frac{\partial^2 c_2}{\partial u^2} \left(\frac{\partial u}{\partial x}\right)^2 + w_e \left(c_{e,2} - u_e \frac{\partial c_2}{\partial u}\right), \tag{9}$$

where the derivatives of c_2 with respect to u have the following expressions

$$\begin{aligned} \frac{\partial c_2}{\partial u} &= \frac{1}{2}\left(-1 + \frac{u}{\sqrt{u^2 + 4\,K_{eq}}}\right), \\ \frac{\partial^2 c_2}{\partial u^2} &= \frac{2\,K_{eq}}{(u^2 + 4\,K_{eq})^{3/2}}. \end{aligned} \tag{10}$$

2.4 Statistics of Reaction Rates

It is clear from (9) and (10) that the reaction rate is only a function of u and its spatial derivative, $u' = \partial u/\partial x$, while u itself is only a function of K. Thus, one can see that $r = r(u(K), u'(K)) = r(K)$. This implies that, if one can derive an analytical solution of (9) for the random rate, r, the moments of r can be obtained by integration in the probability space over which K is sampled.

Alternatively, it would be possible to obtain approximate expressions for the (statistical) moments of r, starting by approximating r in terms of a Taylor's expansion around the (constant) arithmetic mean of K, $K_A(\equiv \langle K \rangle)$

$$r(K) = r(K_A) + \sum_{i=1} \frac{1}{i!} \frac{d^i r}{dK^i}\bigg|_{K=K_A} (K - K_A)^i. \tag{11}$$

The leading terms for the first two moments of r can then be obtained after truncating (11) at second order. Thus, the (second-order) mean rate, $\langle r \rangle$, and the (second-order) variance of reaction rate, σ_r^2, are given respectively by

$$\langle r \rangle \approx r(K_A) + \frac{1}{2}\frac{d^2 r}{dK^2}\bigg|_{K=K_A} \sigma_K^2, \tag{12}$$

$$\sigma_r^2 = \left(\frac{dr}{dK}\bigg|_{K=K_A}\right)^2 \sigma_K^2. \tag{13}$$

An alternative way to find the derivatives involved in (12) and (13) is graphically. For a given set-up it would be possible to find the curve r vs. K. Then the derivatives can be derived graphically.

3 Application Example: 1-D Fixed-step Function

3.1 Explicit Random Solution for the Reaction Rates

The proposed methodology is here applied to the previously described setup problem. The initial and boundary conditions associated with the transport problem are described mathematically as follows:

$$\begin{aligned} &u\,(x, y, z, t = 0) = u^0 \quad x \geq 0 \\ &u\,(x = 0, y, z \in [-a, a], t) = u^0 + \Delta u^0 \quad t \geq 0 \\ &u\,(x = \infty, y, z, t) = u^0 \quad t \geq 0 \end{aligned} \tag{14}$$

The solution of the problem, in the absence of recharge $w_e = 0$, and along one-dimensional lines was provided by Ogata and Banks (1961). The normalized concentration of the component, $u_D = u/\Delta u^0$, can be written in terms of a dimensionless time, $t_D = -\frac{JKt}{\phi x}$ and the *Peclet* number, $\left(Pe = -\frac{JKx}{\phi D_L}\right)$:

$$u_D = \frac{u^0}{\Delta u^0} + \frac{1}{2}\left\{\exp(Pe)\,\mathrm{erfc}\left[\left(\frac{Pe}{4t_D}\right)^{1/2}(1+t_D)\right] + \mathrm{erfc}\left[\left(\frac{Pe}{4t_D}\right)^{1/2}(1-t_D)\right]\right\} \tag{15}$$

It is noted that *Pe* practically ranges between 1 and 100 for flow in aquifers. From (9) and (15), we can obtain an exact, random solution for the dimensionless rate, $r_D(x, y, z, t) = (rx^2)\,/\,(\phi\ D_L \Delta u^0) = f(K_{eqD}, u_D(K), Pe(K), t_D(K))$, as

$$\begin{aligned} r_D \equiv f\,(K) = \frac{1}{2}\frac{K_{eqD}}{\left(u_D^2 + 4\,K_{eqD}\right)^{3/2}} \Bigg\{ &Pe\, e^{Pe}\mathrm{erfc}\left[\left(\frac{Pe}{4t_D}\right)^{1/2}(1+t_D)\right] \\ &-\frac{2}{\sqrt{\pi}}\left(\frac{Pe}{t_D}\right)^{1/2}\exp\left(-\left(\frac{Pe}{4t_D}\right)(1+t_D)^2\right)\Bigg\}^2 \end{aligned} \tag{16}$$

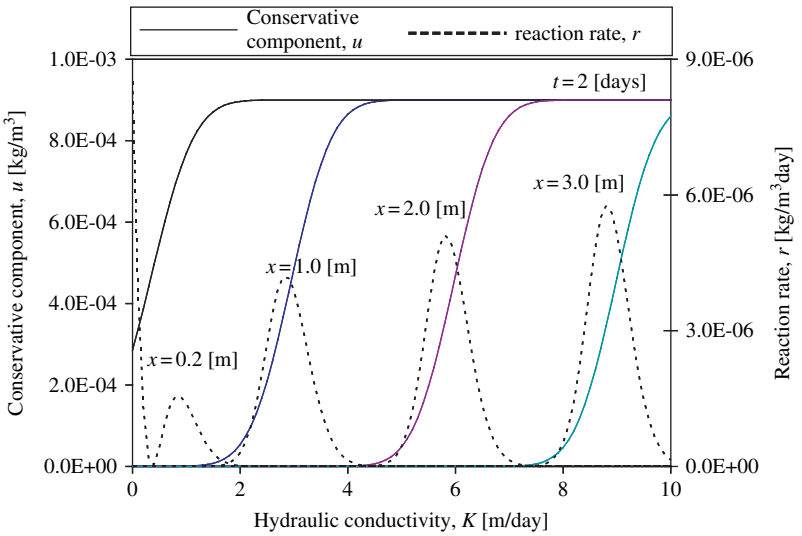

Fig. 1 Dependence of the (random) conservative component, u, and of the rate, r, on K at various distances from the injection line ($x = 0.2$, 1.0, 2.0, 3.0 m) and after a time $t = 2$ days has elapsed since injection. Constant parameters used in the evaluation of (15) and (16) are: $J / \phi = -0.167$, $D_L = 10^{-2}\text{m}^2/\text{day}$, $u^0 = 0.0\,\text{kg/m}^3$, $\Delta u^0 = 9 \times 10^{-4}\,\text{kg/m}^3$, $K_{eq} = 10^{-7}(\text{kg/m}^3)^2$

Here, $K_{eqD} = K_{eq} / (\Delta u^0)^2$. Notice that r_D depends on K through u_D, Pe, and t_D, leading to a highly non-linear behavior. To illustrate this non-linearity, Fig. 1 depicts the dependence of the (random, dimensional) conservative component, u, and of the rate, r, on K at various distances from the injection line ($x = 0.2$, 1.0, 2.0, 3.0 m) and after a time $t = 2$ days has elapsed since injection. Constant parameters used in the evaluation of (15) and (16) are also detailed in the Figure.

From Fig. 1 we see that, for a given time, the rate displays a different behavior at observation points located close to or at some distance from the injection line. Close to the source, the effect of the type of injection, encapsulated by the second term in the parenthesis in (16), results first in the presence of a non-zero value of the rate for $K \to 0$. This is related to dominant diffusive effects in the presence of very low conductivities. This is then followed by a decreasing behavior of the rate with increasing K. This behavior persists until r vanishes and then starts increasing until it reaches a peak. The boundary effect is not felt at larger distances (i.e., at $x = 1$ m the boundary effect is completely lost) so that (15) can be approximated by:

$$u_D = u_{D,0} + \frac{1}{2}\text{erfc}\left[\left(\frac{Pe}{4t_D}\right)^{1/2}(1 - t_D)\right], \tag{17}$$

with $u_{D,0} = u^0/\Delta u^0$. We note that this is also an approximate solution for the transport problem (7) in the presence of different types of boundary conditions,

including (*a*) the third-type boundary condition (Lindstrom et al., 1967), (*b*) the Kreft and Zuber (1978) condition, and (*c*) the constant point source condition (Sun, 1996). The total reaction rate then becomes

$$r = \underbrace{\frac{K_{eqD}}{\left(u_D^2 + 4\,K_{eqD}\right)^{3/2}}}_{A}\ \underbrace{\frac{\phi\,\Delta u^0}{2\pi t}}_{B}\ \underbrace{\left\{\exp\left[-\frac{1}{4D_L t}\left(x + \frac{JKt}{\phi}\right)^2\right]\right\}^2}_{C}. \tag{18}$$

In (18), we identify the product of three terms. The spatial distribution of r is mainly driven by term C. This term is of symmetric shape in x, and peaks at the value $K = -\phi\ x\ /\ (t\,J)$, that is, it increases linearly with x. Term B provides the influence of the maximum with time. Basically, the maximum rate is proportional to t^{-1}. Term A provides a non-linear behavior that basically displaces the maximum towards smaller values of K (as evidenced by Fig. 1). Actually this term is driven by speciation, so that its variation with x is not that relevant. In any case, it is possible to write some bounds for the maximum reaction rate, as follows

$$\frac{K_{eqD}}{\left(\left(u_{D,0} + \frac{1}{2}\right)^2 + 4K_{eqD}\right)^{3/2}}\frac{\phi\,\Delta u^0}{2\pi t} \le r_{\max} \le \frac{K_{eqD}}{\left(u_{D,0}^2 + 4K_{eqD}\right)^{3/2}}\frac{\phi\,\Delta u^0}{2\pi t}. \tag{19}$$

3.2 Statistical Moments of Reaction Rates

Following Section 2.4, we are now in a position to write the following exact expressions for the mean and variance of r_D

$$\left\langle r_D(x,t)\right\rangle = \int_0^\infty f\,(K)\,p_K(K)\,dK, \tag{20}$$

$$\sigma_{rD}^2 = \int_0^\infty \left\{f\,(K) - \langle r_D\rangle\right\}^2 p_K(K)\,dK, \tag{21}$$

where the f function is provided in (16). The results in (17) and (18) are valid regardless of the functional format for the selected pdf. A common choice for the univariate distribution of K is the Log-Normal model, defined by:

$$p_K(K) = p(K) = \frac{1}{\sqrt{2\pi}\,\sigma_Y K}\exp\left\{-\frac{1}{2}\frac{(\ln K - \mu_Y)^2}{\sigma_Y^2}\right\}, \tag{22}$$

where μ_Y and σ_Y are, respectively, the mean and standard deviation of the natural logarithm of K, $Y = ln\ K$. Thus, the mean and variance of the reaction rate can

be obtained after a single quadrature, independently of the shape of the hydraulic conductivity variogram.

It is also important to note that the actual result for mean and variance is independent of the variogram model selected, since it involves only the univariate statistics of K. The main restriction to use the results of (20) and (21) in a single realization is that the parameter a in (14) a has to be much larger than λ_3, in order for ergodic conditions to hold.

4 Evaluation of the Reaction Rate Moments

Figure 2 depicts the dependence of the (ensemble) mean reaction rate, $\langle r \rangle$, on the distance from the line of injection and on time elapsed since injection when Y is Normal with $\mu_Y = 0$ and $\sigma_Y^2 = 1$. The constant input parameters are those of Fig. 1. The mean rate displays a non-monotonous behavior. It is characterized by a local maximum that (a) decreases in magnitude and (b) is displaced towards larger distances with time. The local maximum is then followed by a decreasing limb, whose rate of decay decreases with time.

The effect of the dispersion coefficient on $\langle r \rangle$ at a given time is illustrated in Fig. 3. Increasing the rate of mixing, as implied by large values of D_L, produces an increase of the local value of the mean reaction rate. The latter displays a larger spatial persistence for the largest D_L examined, thus evidencing the importance of this term in a geochemically active system. With the only exception of locations at

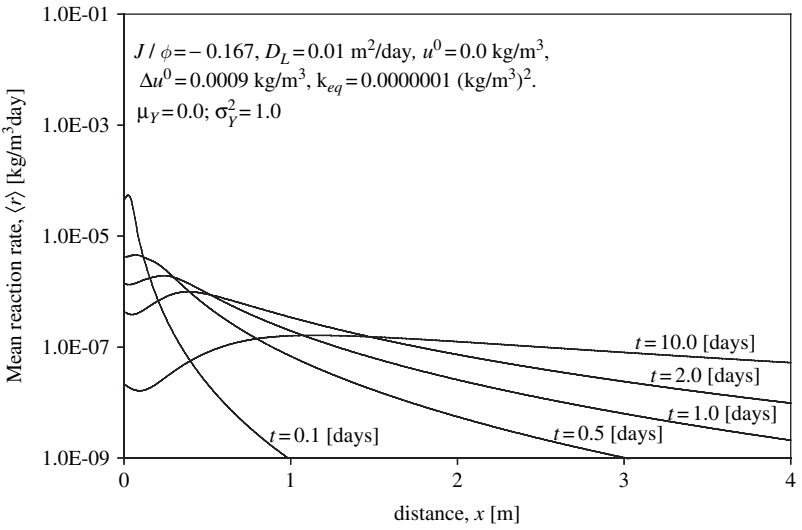

Fig. 2 Dependence of the (ensemble) mean reaction rate, $\langle r \rangle$, on the distance from the line of injection and on time elapsed since injection when Y is Normal with $\mu_Y = 0$ and $\sigma_Y^2 = 1$

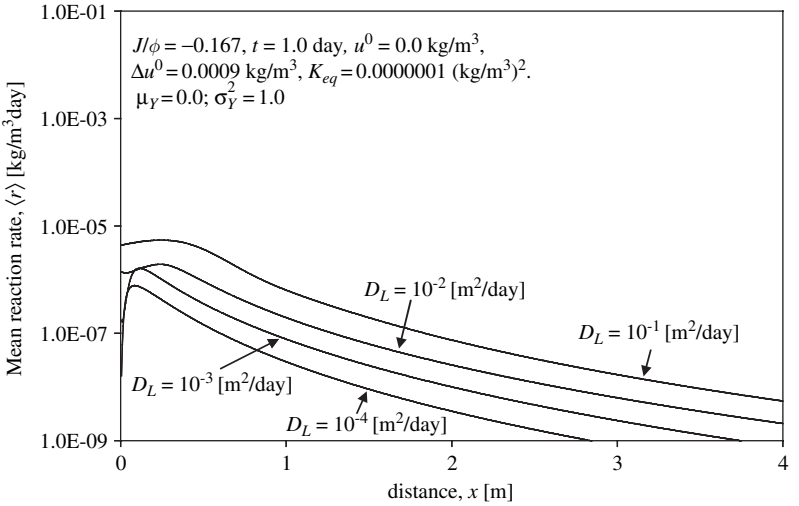

Fig. 3 Dependence of the (ensemble) mean reaction rate, $\langle r \rangle$, on the distance from the line of injection and on D_L for a fixed time when Y is Normal with $\mu_Y = 0$ and $\sigma_Y^2 = 1$

short distances from the source line, each increase of D_L of an order of magnitude produces a local increase of $\langle r \rangle$ of about half order of magnitude.

The standard deviation, σ_r, associated with the mean reaction rate is shown in Fig. 4 as a function of distance and time, when Y is Normal with $\mu_Y = 0$ and $\sigma_Y^2 = 1$. We start by noting that the σ_r is of the same order of magnitude as $\langle r \rangle$ for very short

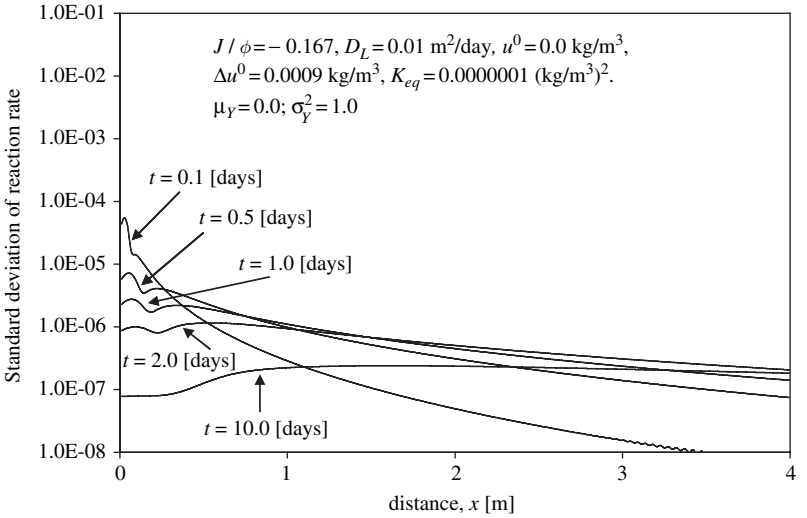

Fig. 4 Standard deviation of the reaction rate [in kg/m^3/day] versus distance from the line of injection and for different times. Y is Normal with $\mu_Y = 0$ and $\sigma_Y^2 = 1$

distances from the injection line. The rate of decay of σ_r with x is generally lower than that of $\langle r \rangle$. It follows that for the investigated time intervals σ_r is generally larger than $\langle r \rangle$ and much more so as x increases. This suggests that this type of structured heterogeneity results in coefficients of variations of the local rate generally larger than 100% for short times and/or distances. Since the system we analyze displays a high geochemical activity precisely in the range of short times and distances, we can conclude that uncertainty in the vertical distribution of hydraulic conductivity has a large negative influence on the predictability of the behavior of the system within regions where significant reaction rates occur.

As opposed to the mean rate, σ_r displays a local minimum that is located close to the source line and travels from the origin relatively slowly with time. In the example considered, σ_r displays a primary and a secondary peak, both of them decreasing with time. While the location of the primary peak is largely insensitive to the elapsed time (controlled by the boundary conditions), the position of the secondary peak travels along x as time increases.

The dependence of the spatial distribution of $\langle r \rangle$ on the variance of Y for times $t = 0.5$ and 2 days is depicted in Fig. 5. Corresponding depictions documenting the behavior of σ_r are offered in Fig. 6. It can be noted that, in general, both $\langle r \rangle$ and σ_r tend to increase with σ_Y^2. This tendency is less pronounced as time increases. It is also interesting to note that $\langle r \rangle$ and σ_r are relatively insensitive on the heterogeneity of the underlying log-conductivity field close to the line source. The distance within which this behavior persists increases with elapsed time.

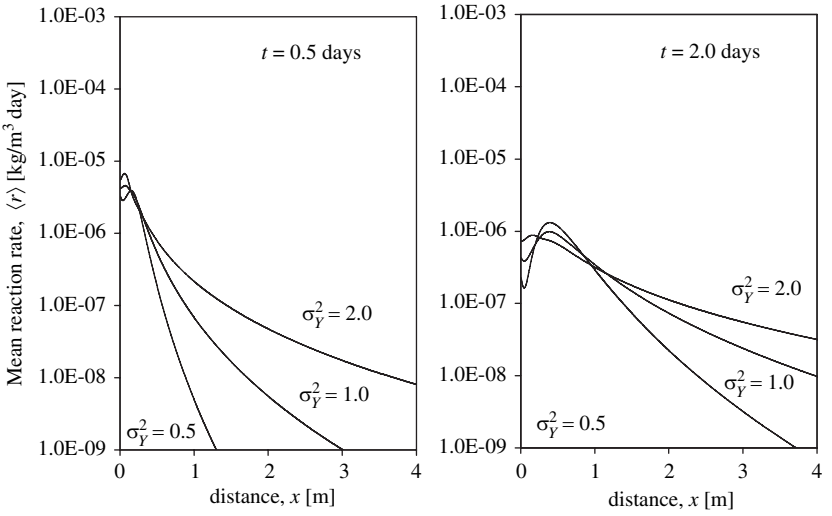

Fig. 5 Impact of the variance of Y on the spatial distribution of $\langle r \rangle$ versus travel distance, for times $t = 0.5$ and 2 days. Constant parameters used are: $J / \phi = -0.167$, $D_L = 10^{-2}\text{m}^2/\text{day}$, $u^0 = 0.0\,\text{kg/m}^3$, $\Delta u^0 = 9 \times 10^{-4}\,\text{kg/m}^3$, $K_{eq} = 10^{-7}(\text{kg/m}^3)^2$, $\mu_Y = 0.0$

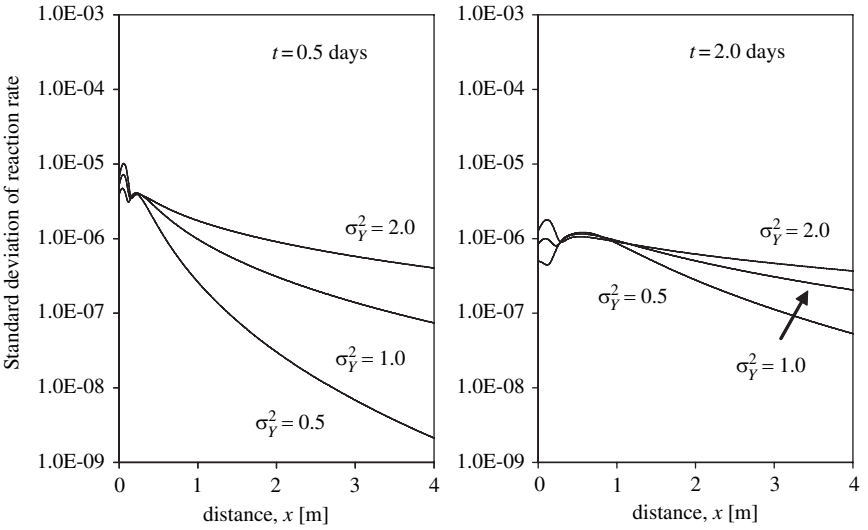

Fig. 6 Dependence of the variance of Y on the spatial distribution of σ_r versus distance for times $t = 0.5$ and 2 days. Constant parameters used are: $J / \phi = -0.167$, $D_L = 10^{-2}\,\mathrm{m^2/day}$, $u^0 = 0.0\,\mathrm{kg/m^3}$, $\Delta u^0 = 9 \times 10^{-4}\,\mathrm{kg/m^3}$, $K_{eq} = 10^{-7}(\mathrm{kg/m^3})^2$, $\mu_Y = 0.0$

5 Conclusions

We consider transport of reactive species in an anisotropic correlated random hydraulic conductivity field, with perfect correlation in the horizontal plane, while the vertical integral scale is finite. Flow is uniform and takes place in the x-direction. Uncertainty in the (vertical) distribution of the advective velocity causes the reaction rate to become a Spatial and Temporal Random Function. The low-order statistical moments (mean and variance) of the reaction rate for given space-time coordinates can be obtained in terms of a simple quadrature in probability space of hydraulic conductivity.

Our results highlight that, in general, both the mean and standard deviation of the reaction rate tend to increase with the level of heterogeneity of the hydraulic conductivity field. The coefficient of variation of the rate of reaction is always larger than 100%, thus evidencing the negative impact of uncertain hydraulic conductivity distribution on the predictability of such geo-chemical processes.

This work is a first stage toward advancing in the study of the evaluation of reaction rates in complex mutispecies transport of reactive species in heterogeneous media. This problem has profound implications in natural or enhanced attenuation systems. At larger distances it will be necessary to consider more realistic variogram models with finite correlation scales as well as to incorporate the effect of transverse dispersion.

References

Dentz M, Carrera J (2003) Effective dispersion in temporally fluctuating flow through a heterogeneous medium, Physical Review E, 68 (3): Art. No. 036310

De Simoni M, Carrera J, Sanchez-Vila X, Guadagnini A (2005) A procedure for the solution of multicomponent reactive transport problems, Water Resour Res, 41(11): Art. W11410

Gramling CM, Harvey CF, Meigs LC (2002) Reactive transport in porous media: A comparison of model prediction with laboratory visualization. Environ Sci Tech 36(11): 2508–2514

Kreft A, Zuber B (1978) On the physical meaning of the dispersion equation and its solutions for different initial and boundary conditions, Chem Eng Sci 33: 1471–1480

Lindstrom FT, Haque R, Freed VH, Boersma L (1967) Theory on the movement of some herbicides in soils: Linear diffusion and convection of chemicals in soils, J. Environ Sci Technol 1: 561–565

Matheron G, DeMarsily G (1980) Is Transport In Porous-Media Always Diffusive - A Counterexample, Water Resour Res 16 (5): 901–917

Ogata A, Banks RB (1961) A solution of the differential equation of longitudinal dispersion in porous media, U. S. Geol. Surv. Prof. Paper 411-A

Sun NZ (1996) Mathematical Modeling of Groundwater Pollution, Springer-Verlag, NY